Case Studies in Construction Materials 15 (2021) e00760

Contents lists available at ScienceDirect

Case Studies in Construction Materials

journal homepage: www.elsevier.com/locate/cscm

Utilisation of dewatered extracted soil in concrete blocks produced with Portland cement or alkali-activated slag: Engineering properties and sustainability

Wenjie Luo [a], Shu Liu [a,b], Yuan Jiang [a], Xiwen Guan [a], Yunfeng Hu [c], Dongdong Hu [c], Bo Li [a,b,*]

[a] Department of Civil Engineering, University of Nottingham Ningbo China, 199 Taikang Road, Ningbo 315100, China
[b] Key Laboratory of Carbonaceous Wastes Processing and Process Intensification of Zhejiang Province, University of Nottingham Ningbo China, Ningbo 315100, China
[c] Ningbo Transportation Engineering Construction Group Co. Ltd., Ningbo 315100, China

ARTICLE INFO

Keywords:
Dewatered extracted soil
Concrete block
Cement-based
Alkali-activated slag
Life cycle assessment

ABSTRACT

Disposal of soil from foundation excavation in the construction industry has been recognised as a critical challenge for environmental protection. This study investigates the feasibility of incorporating dewatered extracted soil (DES) in concrete blocks manufactured with ordinary Portland cement (OPC) or alkali-activated slag (AAS). The physical and engineering properties, including bulk density, water absorption, compressive strength and flexural strength, of the concrete blocks with different contents of DES were investigated. Scanning electron microscope (SEM) analysis was also conducted to investigate the microstructure of the blocks. The results indicate that replacing sand by DES can enhance the physical and mechanical properties of the concrete blocks. The optimal replacement ratios are 30% for the OPC concrete blocks (OPCCB) and 20% for the AAS concrete blocks (AASCB). At the optimal replacement ratios, the densities of OPCCB and AASCB are 10.5% and 19.6% higher than those without DES, respectively, while the water absorption ratios are 38.0% and 48.7% lower than those without DES, respectively. Consequently, the 28-day compressive and flexural strengths for both blocks were increased by over 100%. The SEM photographs indicate that the improvements are attributed to the densification of the structure. However, further increasing the incorporation ratio of DES increases the surface area of total aggregates and requires more OPC or AAS to bind them, which consequently weakens the properties of concrete blocks. Besides, the strength of concrete blocks with AAS is around 2 times that with the same amount of OPC, indicating that AAS is more effective in improving the strength of concrete blocks. Moreover, a cradle-to-gate life cycle assessment (LCA) was performed to analyse the energy consumption and embodied carbon of the concrete blocks. The results indicate that AASCBs exhibits superior environmental sustainability over both conventional fired clay bricks and OPCCBs. Results in this study can help promote the application of DES in producing green concrete blocks.

* Corresponding author at: Department of Civil Engineering, University of Nottingham Ningbo China, 199 Taikang Road, Ningbo 315100, China.
E-mail address: bo.li@nottingham.edu.cn (B. Li).

https://doi.org/10.1016/j.cscm.2021.e00760
Received 9 August 2021; Received in revised form 21 October 2021; Accepted 23 October 2021
Available online 25 October 2021
2214-5095/© 2021 The Author(s). Published by Elsevier Ltd. This is an open access article under the CC BY-NC-ND license (http://creativecommons.org/licenses/by-nc-nd/4.0/).

1. Introduction

Brick is one of the most widely used building materials in the construction industry [1]. Annual production of bricks has reached 1.83 trillion units in 2017, and is estimated to be increased to 2.76 trillion units by 2027 [2]. However, the conventional brick production technology consumes a huge amount of energy and emits a significant quantity of carbon dioxide into the environment. For instance, producing 1 ton of fired clay bricks (FCB) consumes 4890 MJ of energy, which is mainly associated with its sintering manufacturing process [3]. As a result, the non-sintering concrete block production technology has attracted increasing attention due to its advantages in energy efficiency and environmental sustainability [2].

Construction and demolition wastes (CDWs) have been recycled and reused as construction materials. Arulrajah et al. [4] demonstrated that the pavement base/subbase with recycled concrete aggregate, crushed bricks and waste excavation rock exhibits satisfactory physical properties and shear strength. Suluguru et al. [5] adopted waste concrete and brick as a partial substitution of soil for ground improvement. After immersion in seawater, nitric acid and hydrochloric acid, the soil with waste concrete showed better chemical resistance as verified by means of aggregate impact value, X-ray diffraction and stereo microscopy. Suluguru et al. [6] assessed the impact resistance of various types of CDWs, and reported that crushed marble tiles, normal-strength concrete and high-strength concrete can meet the engineering requirements of subbase materials. Chen et al. [7] studied the environmental impact of leachate caused by RCA used in subgrade soil, and concluded that soils with a higher clay content delayed the propagation of alkaline leachate. For recycled concrete products, the existing studies primarily focused on the use of recycled aggregates and powders in concrete block production [8–11], and demonstrated that they can be successfully utilised as coarse or fine aggregates in concrete blocks. Dewatered extracted soil (DES) from construction activities takes up a large scale of CDW. With more than 700 million tons of extracted soils and rocks generated each year in the European Union (EU), initiatives have been taken to guide construction sectors toward reusing them as potential resources [12]. Particularly, many mountainous countries in EU produce an enormous amount of extracted wastes for their tunneling constructions. Disposal and reuse of DES remain to be a severe challenge to the environment and construction industry. To tackle this issue, Meegoda et al. [13] utilised contaminated soil in concrete block production, and found the concrete blocks with soil possess satisfied engineering properties, high cost efficiency and eco-friendliness. Hago et al. [14] investigated the properties of concrete blocks with 60% sand replaced by contaminated soil, and reported that there was no significant deterioration in their mechanical properties and durability. Lesovik et al. [15] assessed the engineering properties and durability of green concrete blocks incorporated with soil and rocks extracted from ore mining, and demonstrated that the concrete blocks incorporated 20% sandy clay can attain a compressive strength of 20 MPa. Korte and Brouwers [16] optimised the mix formulations of hollow concrete blocks with humus-rich peat soil and sand soil on the basis of the packing density theory. Reddy and Gupta [17] pointed out that reduction in mechanical strength of concrete blocks with high fineness of soil was caused by the requirement on high water content. In general, the above-mentioned studies demonstrated that various types of extracted soils can be used as appropriate substitutions of aggregates in concrete blocks. Nevertheless, the excavated soil from the pile foundation construction has not yet been broadly explored in concrete block production.

Cement used in concrete blocks is the main source of high energy consumption and carbon emission. For instance, the carbon dioxide emitted by the cement manufacturing industry accounts for 5–8% of the world's CO_2 emission [18]. Apart from the greenhouse gas emission, it is commonly accompanied by emission of atmospheric pollutants (e.g. CO, NO_x and SO_2) [19]. Therefore, it is urgent to replace OPC with novel binders for the sustainable development of construction industries. Hence, alkali-activated materials (AAMs) have been developed as the alternative binder, which can be synthesised via the reaction between alkaline activators and aluminate/silicate based precursors, e.g. metakaolin [20], fly ash [21–24], ground granulated blast-furnace slag [24] and their mixtures [25–29]. The alkaline activators comprise soluble natrium/kalium silicate and alkaline hydroxide. In the alkaline environment, the aluminosilicate dissolved from precursors transforms into growing gels made up of the tetrahedral units such as SiO_4, AlO_4^- and their integrates. These tetrahedral units are linked by sharing oxygen atoms, forming frameworks inside the AAMs during the reaction process [29]. AAMs have been recognised as the eco-friendly binder due to its lower carbon emissions (250–450 kg/t), which can decrease CO_2 emission by up to 67% [30]. Ramagiri et al. [31] pointed out that global warming potential of OPC-based concrete is 40–100% higher than that of alkali-activated concrete. On the other hand, AAMs have been proved to be suitable for improving the physical and mechanical properties of concrete blocks as binder [32]. Abdullah et al. [33] tested the physical, mechanical and durability properties of fly ash based alkali-activated concrete blocks, and recommended the optimal FA-to-sand ratio to be 0.2 to achieve the highest compressive strength (17 MPa) and the lowest water absorption (3.7%) for concrete blocks. Ren et al. [34] utilised recycled concrete fines (RCF) and recycled concrete powder (RCP) in alkali-activated slag concrete blocks, and concluded that replacing 60–80% aggregate by RCF and 10–30% slag by RCP can optimise the properties of AAS concrete blocks, respectively. However, few studies have been carried out on the use of excavated soils in alkali-activated concrete blocks. Consequently, there is a lack of comparative studies to evaluate the energy consumption and carbon emission of OPC and AAS based concrete blocks.

Therefore, this paper investigates the feasibility of using excavated soil in OPC and AAS concrete block production through comparing their engineering properties. Fine aggregates in concrete blocks are replaced by various amounts of dewatered extracted soils. The density, water absorption capacity, compressive strength and flexural strength of the concrete blocks are measured, followed by microstructure characterisation by Scanning Electron Microscope (SEM). A cradle-to-gate life cycle assessment (LCA) is implemented to quantify energy consumption and embodied carbon of blocks, aiming at contrastively demonstrating the sustainability of the OPC or AAS concrete blocks over the conventional fired clay bricks.

2. Experimental programme

2.1. Raw materials

In this study, dewatered extracted soil (DES), ordinary Portland cement (OPC), ground granulated blast-furnace slag (GGBS), river sand, and coarse aggregate were used as the raw materials for preparing concrete blocks. As shown in Fig. 1, the DES, as the waste of cast-in-situ bored pile construction, was collected from a highway construction site in Ningbo, China. The 42.5$^{\#}$ OPC in accordance with GB 175 [35] and S95 GGBS in accordance with GB/T 18046 [36] were used as the binders. Their chemical compositions and particle distributions are shown in Table 1 and Fig. 2, respectively. The median particle sizes (D50) of the OPC, GGBS and soil are 22.013 μm, 12.279 μm, and 23.502 μm, respectively. Therefore the soil is classified as clay in line with BS ISO EN [37]. The combined determination method for liquid and plastic limits performed as per JTG 3430-2020 [38] indicates that the liquid limit, plastic limit and plasticity index of DES are 29.75%, 19.41% and 10.34%, respectively. X-ray diffraction (XRD) tests were conducted at 2θ degree from 3° to 70° with Cu-Kα radiation (λ = 1.54 Å) to investigate the mineralogical composition of the DES. The XRD results shown in Fig. 3 reveal that quartz, kaolinite, illite and smectite are the main crystals phases. In terms of river sand, locally available sand was used and its gradation shown in Fig. 2 meets the requirements of GB/T 14684 [39]. The specific gravities of sand and DES are 2.44 and 2.38, respectively. The particle size of coarse aggregate ranges from 5 mm to 10 mm. The mixed solution of water, sodium hydroxide (98%, AR) and commercially available water glass (WG) consisting of 8.3% Na_2O, 26.8% SiO_2 and 64.9% H_2O by mass was used as the activator.

2.2. Test plan

DES was used to partially replace sand in the concrete blocks. The effect of soil replacement ratio on the properties of ordinary Portland cement concrete blocks (OPCCB) and alkali-activated slag concrete blocks (AASCB) was investigated. The mix formulations are listed in Table 2, where C stands for OPCCB, A stands for AASCB, and the numbers behind them represent soil replacement ratios in percentage. The masses of fine aggregates (i.e., sand and soil) and binders (i.e., OPC and AAS) remained constant, aiming to investigate the influence of soil content on the properties of concrete blocks. Moreover, it should be noticed that the water was composed of two parts due to their different functions. The proportion of water for hydration reaction remained constant. Otherwise, compensatory water was added to consider the water absorption of fine aggregates. Its amount was assumed equal to saturated surface-dry (SSD) moisture contents in aggregates. The SSD moisture content of soil was determined with the drying rate method [40]. Specifically, DES was adequately dried first, followed by mixing with water amounting for 6–33% of its dry mass. This mixture was sealed for soakage for at least 24 h and then placed on an electronic scale under 150 ℃. The changing masses were recorded every 30 min. The test would end when the mass changing rates became less than 0.01%/hour. The moisture content (C), desiccation rate (R) and derivate rate (D) therefore can be obtained according to Eqs. (1)–(3). The maximum D would be taken as the SSD moisture content of soil. The test results shown in Fig. 4 denote the SSD water content of DES is 25.5%. The SSD moisture content of river sand was tested to be 0.26% through GB/T 14684 [39].

$$C = \frac{m_i - m_{dry}}{m_{dry}} \tag{1}$$

$$R = \frac{m_i - m_{i+a}}{a} \tag{2}$$

$$D = \frac{R_i - R_{i+a}}{a} \tag{3}$$

where m_i and $m_{(i+\alpha)}$ are the sample masses at time i and $i + \alpha$, respectively. α is the time spacing in hour. m_{dry} is the sample mass in a

Fig. 1. Dewatered soil extracted from foundation excavation.

Table 1
Chemical compositions of OPC, GGBS and soil.

Compound	Chemical compositions (%)		
	OPC	GGBS	Soil
SiO_2	19.83	29.02	62.63
Al_2O_3	5.66	13.97	15.45
Fe_2O_3	3.50	0.38	7.72
CaO	62.43	43.52	5.33
MgO	2.17	8.97	2.45
K_2O	1.19	0.51	3.31
Na_2O	N/A	0.07	N/A
TiO_2	N/A	N/A	1.22
SO_3	4.08	0.42	N/A

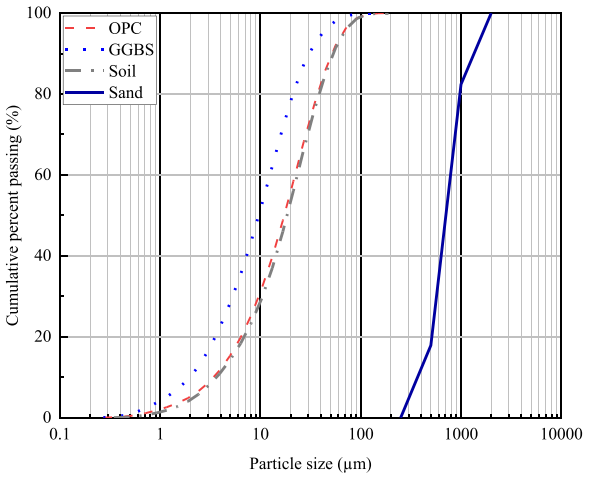

Fig. 2. Particle size distributions of OPC, GGBS, soil and sand.

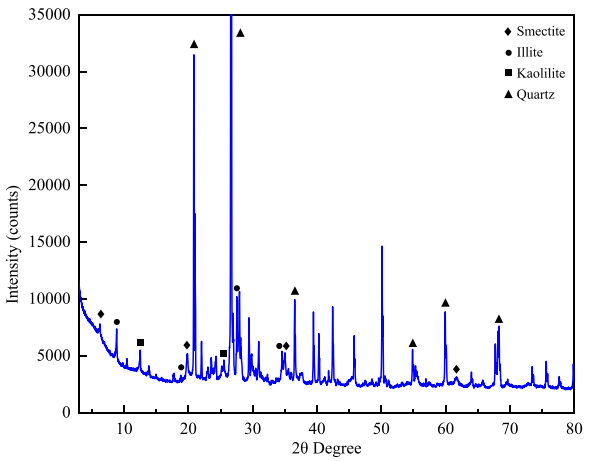

Fig. 3. XRD results of DES.

completely dry condition. R_i and $R_{(i+\alpha)}$ are drying rates at time i and $i + \alpha$, respectively.

2.3. Sample preparation

The cement (or slag), dried DES, sand, and gravel were first blended in a planetary mixer for 2 min, followed by adding the water or alkaline activator. The activator was prepared through blending the water glass, sodium hydroxide pellets, and water, and was cooled

Table 2
Mix formulations of concrete blocks in mass proportion.

Mix	OPC/GGBS	Gravel	Sand	Soil	Water		NaOH	WG
					Hydration	Compensatory		
C0	1	7.5	2.50	0	0.3	0.12	N/A	N/A
C10			2.25	0.25		0.17	N/A	N/A
C20			2.00	0.50		0.22	N/A	N/A
C30			1.75	0.75		0.27	N/A	N/A
C40			1.50	1.00		0.32	N/A	N/A
A0	1	7.5	2.50	0	0.3	0.12	0.083	0.152
A10			2.25	0.25		0.17	0.083	0.152
A20			2.00	0.50		0.22	0.083	0.152
A30			1.75	0.75		0.27	0.083	0.152

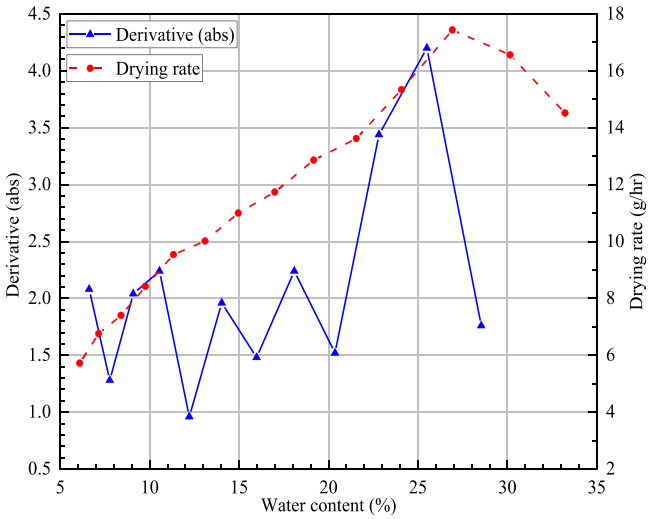

Fig. 4. SSD moisture content of DES.

down to room temperature in advance. The mixture was mixed for another 5 min before adding to the steel moulds as shown in Fig. 5 (a). The wet mixtures were cast into steel moulds with an interior dimension of 200 mm × 100 mm× 60 mm and compressed into blocks with loading as shown in Fig. 5(b). The compressive loading gradually increased to 400 kN at a rate of 6 kN/s. The fabricated block samples were covered with plastic films and cured at room temperature for 1 day as seen in Fig. 5(c). Afterwards, the samples were demoulded and placed in a standard curing chamber with a constant temperature of 20 °C and a relative humidity of 95%.

(a) Mixed green mixture (b) Forming under compression (c) Prepared samples under curing

Fig. 5. Concrete blocks preparation procedure.

2.4. Test methods

Bulk density and water absorption of concrete blocks were measured according to ASTM C642 [41]. Compressive strength and flexural strength of concrete blocks were determined according to GB/T 2542 [36]. The loading rate for the compressive strength test (Fig. 6(a)) was 2.4 kN/s, whilst 3-point flexure test (Fig. 6(b)) was performed over a span of 160 mm at a loading rate of 100 N/s. The SEM samples were extracted from the middle section of crushed concrete blocks, and their hydration was terminated by immersing in isopropanol for 24 h. Afterwards, the samples were desiccated at 40 °C in a vacuum oven for 24 h and were coated with 5 nm thick gold in argon atmosphere. SEM characterisation was performed at voltages of 5 kV and 7 kV for the OPC and AAS concrete blocks, respectively.

2.5. Life cycle assessment (LCA)

LCA was carried out based on the guideline promulgated by ISO 14040 and ISO 14044 [42,43]. LCA can be split into three specific methodologies via delimiting different scopes [2], namely cradle-to-grave, cradle-to-gate and cradle-to-cradle. Among them, the cradle-to-gate LCA was adopted in this study. The open-access software openLCA 1.10.3 was used to exercise the LCA and compare the environmental impacts of OPCCB, AASCB and the conventional fired clay brick (FCB).

3. Results and discussion

3.1. Bulk density

Fig. 7 plots the bulk density of the OPCCB and AASCB against the soil replacement ratios. The bulk density of concrete blocks first increases as the soil replacement ratio increases, followed by a slight decrease. Compared with the conventional concrete blocks, the bulk densities of OPCCB and AASCB are increased by up to 10.5% and 19.6% due to the incorporation of the DES, respectively. This could be attributed to the improvement of the aggregate packing status since DES could fill the voids among the aggregates [44,45]. However, excessive DES would adversely affect the packing status and therewith decrease the volume density [44,45]. For instance, increasing the soil replacement ratio from 30% to 40% decreases the bulk density of OPCCB by 2.0%. This is probably caused by the voids created by the agglomerated soil in concrete blocks. The optimum soil replacement ratio of OPCCB (i.e., 30%) is larger than that of AASCB (i.e., 20%), which means that more DES is required by OPCCB to optimise its packing status. In addition, there is a more significant improvement in bulk density for AASCB than OPCCB. This is because the particle size of the DES is similar to that of OPC, but larger than that of GGBS, suggesting that the incorporation of GGBS could lead to a more uniform grading condition over a larger dimension span for the AASCB than the OPCCB.

3.2. Water absorption

Fig. 8 demonstrates the water absorption of OPCCB and AASCB with different soil replacement ratios. The water absorption of both types of concrete blocks decreases as the soil replacement ratio increases, followed by a slight increase as the soil replacement ratio exceeds the optimum value. In general, the water absorption of OPCCBs with DES is decreased by 13.6–38.0% as compared to that without DES. More significantly, the water absorption of AASCB with DES is decreased by 22.8–48.7% as compared to that without soil. This indicates that the addition of DES is able to decrease the water absorption of OPCCB and AASCB, which is mainly caused by the refinements in particle packing and mixture compaction [44,46]. It is also found that the variation of water absorption is inversely correlated to bulk density change of concrete blocks with various soil replacement ratios in Section 3.1. Moreover, the water absorptions of AASCB are lower than those of OPCCB with the same soil replacement ratio. Incorporating 20% DES decreases the water

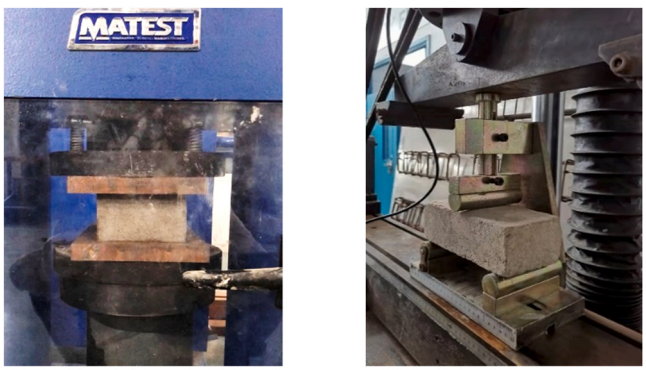

(a) (b)

Fig. 6. Photographs of (a) compression test and (b) flexural test of concrete blocks.

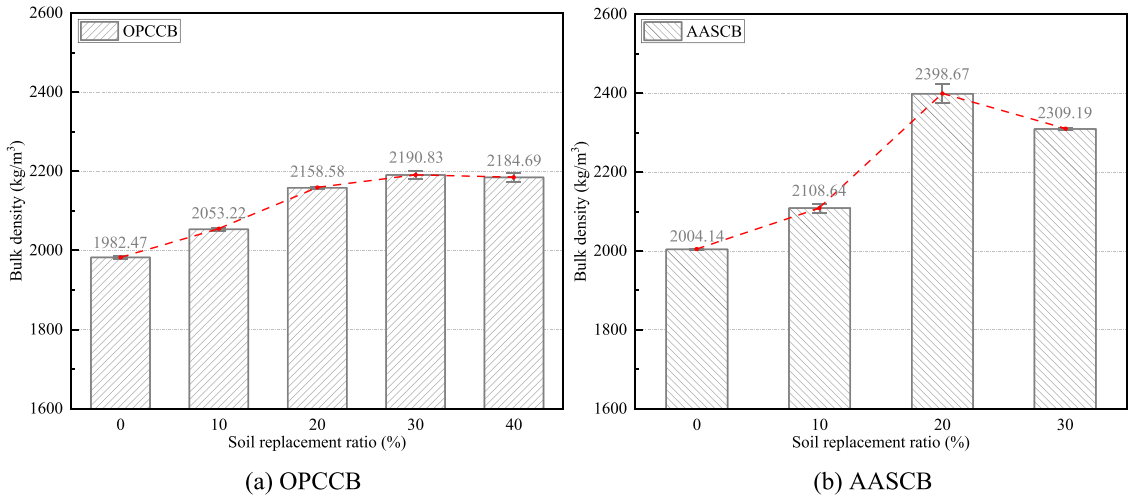

Fig. 7. Bulk density of concrete blocks with different soil replacement ratios.

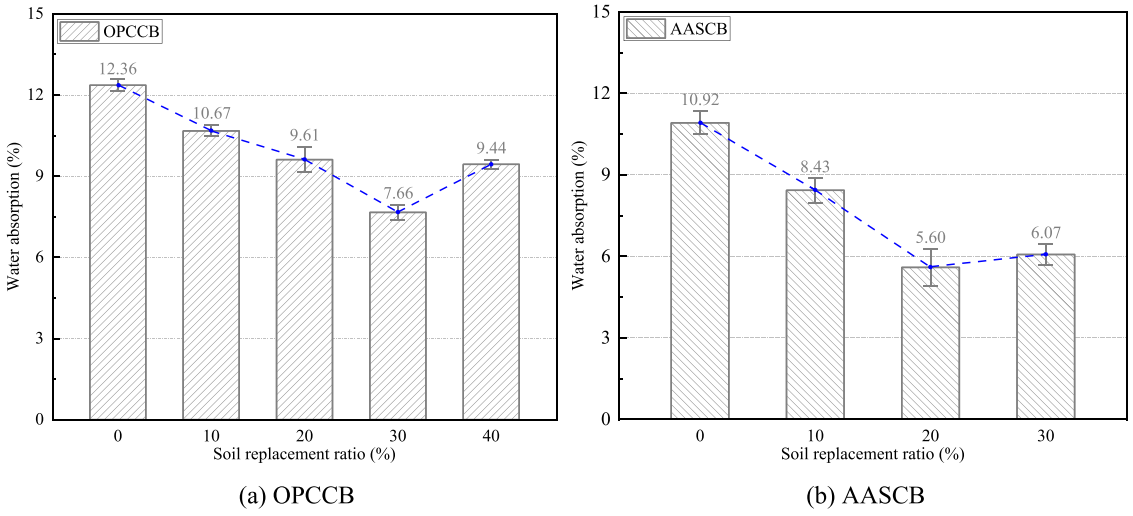

Fig. 8. Water absorption of concrete blocks with different soil replacement ratios.

absorption of OPCCB and AASCB by 22.5% and 45.5%, respectively. It indicates that the use of soil is more effective in reducing the water absorption of AASCBs. The optimum soil replacement ratios of OPCCB and AASCB are 30% and 20%, respectively.

3.3. *Compressive strength*

Fig. 9 shows the compressive strength of OPCCB and AASCB against the soil replacement ratio. The compressive strength of concrete blocks first increases with the amount of soil, followed with a reduction after reaching the optimum replacement ratio. For both concrete blocks with OPC and AAS, replacing 10% of fine aggregate by DES has a marginal impact on their compressive strengths. Further increasing the replacement ratio of soil to 20% significantly improves the compressive strength of concrete blocks. For instance, compared to that without soil, the 7-day and 28-day compressive strengths of OPCCB are increased by 54.25% and 69.59% when the amount of soil raises from 10% to 20%, respectively. As seen in Fig. 9, the optimum amounts of soil in concrete blocks with OPC and AAS are 30% and 20%, respectively. This replacement ratio of soil is consistent with the previous studies [47,48]. The concrete blocks with OPC and AAS achieve maximum 28-day compressive strengths of 21.94 MPa and 50.13 MPa, respectively. As compared with the concrete blocks without DES, the maximum compressive strengths of concrete blocks with soil are doubled. The overall tendency agrees well with that of the bulk density, which is in consistent with the findings reported by Tripura et al. [49]. As seen in Fig. 2, the DES used in this study has analogous particle size distribution to that of OPC, which has an evident filling effect on the concrete blocks [50]. However, excessive soil increases the surface area of total aggregates, which requires more binders (e.g., cement or AAS paste) to bond or coat the aggregates. Insufficient binder may cause the loss of adhesion between aggregates [44]. For

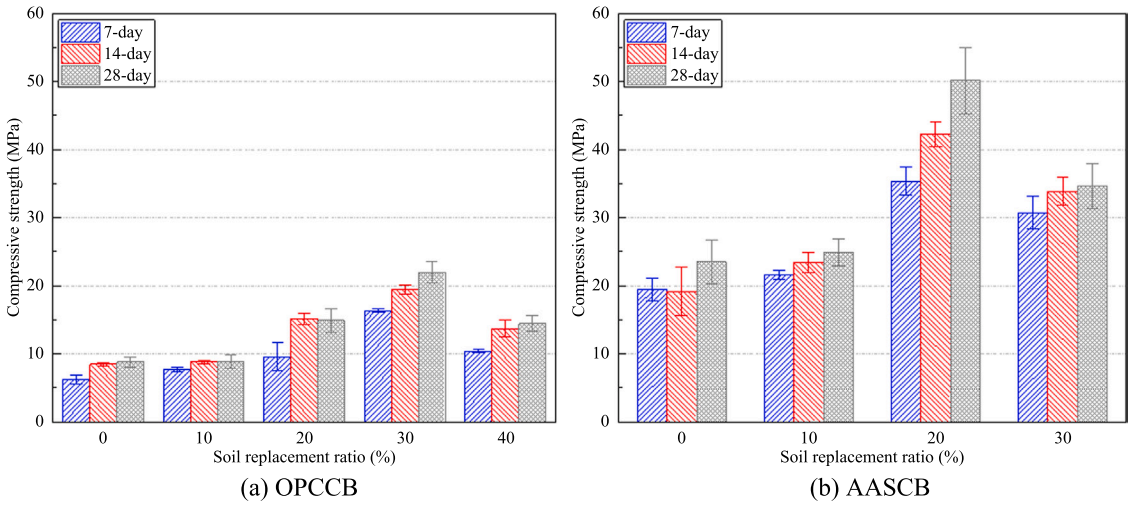

Fig. 9. Compressive strength of concrete blocks with different soil replacement ratios.

instance, the 28-day compressive strength of OPCCB and AASCB are decreased by around 30% when increasing the soil content by 10% after the optimal replacement ratio. It can be noticed that the optimal replacement ratio of soil for AASCB is lower than that for OPCCB, which indicates that less soil is needed for AASCB to achieve the highest strength. This can be explained by the micro-filling effect of slag since its particle size is smaller than that of OPC [51].

The compressive strength of AASCB is generally higher than that with OPCCB when an identical amount of DES is contained. For the concrete blocks with 10% DES replacement, the 28-day compressive strength of AASCBs is around 2.4 times that of OPCCBs. Increasing the soil replacement ratio to 20% increases the difference in compressive strength of concrete blocks produced with OPC and AAS. At the DES replacement ratio of 20%, the compressive strength of AASCB is 3.37 times that of OPCCB. It proves that the AAS is more effective in enhancing the strength of concrete blocks with DES [52,53].

3.4. Flexural strength

Fig. 10 shows the flexural strength of OPCCB and AASCB with different soil replacement ratios. Similar to the compressive strength, the flexural strength of concrete blocks with OPC and AAS first increases with the amount of DES, followed by a decrease as the soil content exceeds the optimum ratio. Incorporating a small amount of DES (e.g., no more than 20% in OPCCB and 10% in AASCB) increases the flexural strength of concrete blocks by around 20%. Further increasing the replacement ratio of sand conspicuously enhances the flexural strength of concrete blocks. For instance, the flexural strength of OPCCB is increased by 102.9% when 30% of sand is replaced by DES. Similarly, the flexural strength of AASCB is doubled after incorporating 20% of DES. This indicates that DES has a filler effect in densifying the concrete blocks [51]. When the soil content exceeds the optimum replacement ratio, the flexural

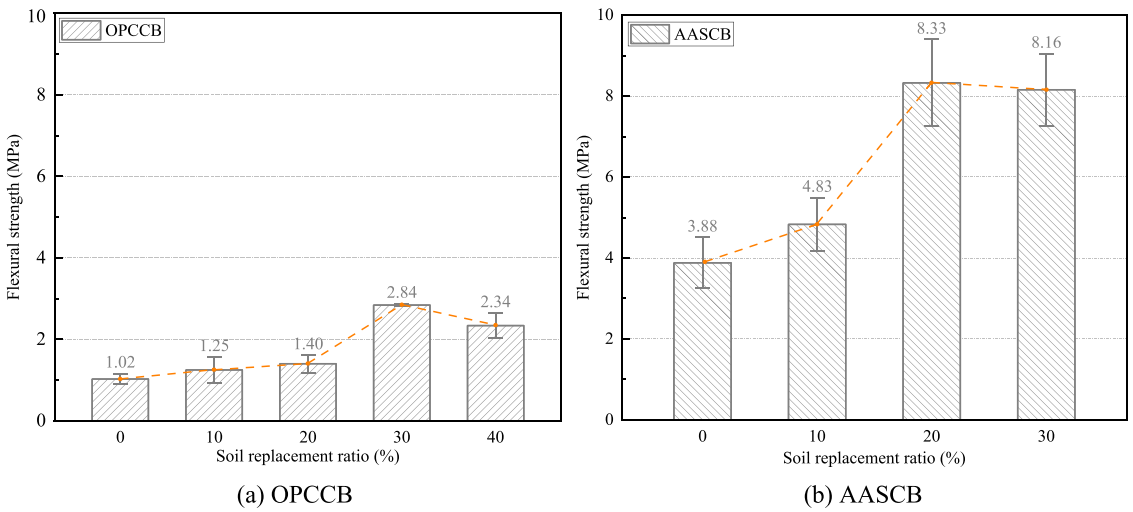

Fig. 10. Flexural strength of concrete blocks with different soil replacement ratios.

strengths of concrete blocks with OPC and AAS decrease by 17.61% and 2.04%, respectively. It is caused by the increased surface area of aggregates after incorporating the DES, which requires more binder to coat their surfaces. Furthermore, the addition of excessive soil also deteriorates the packing status of aggregates, which negatively affects the flexural strength of concrete blocks. The AASCBs generally show the higher flexural strength than OPCCBs regardless of the DES content. At the same soil replacement ratio, the flexural strength of AASCB approximates to be 4 times that of OPCCB. It reveals that there exists higher enhancement efficiency of flexural strength in adding soil into AAS, resulting from the well-refined packing condition brought by the fine size of GGBS [51].

3.5. Scanning electron microscopy (SEM)

Fig. 11 shows the SEM images of OPCCB and AASCB with various amounts of DES. The details of mixes C0, C30, A0 and A20 can be referred to Table 2. The OPCCB with DES (Fig. 12(b)) exhibits fewer pores than that without DES (Fig. 12(a)), as the fine soil can fill up most of them [54]. The pores in OPCCB without DES seem to be larger than those in the concrete block with DES. Ten typical major pores were outlined and measured for Mixes C0 and C30, respectively. The statistical results tabulated in Table 3 demonstrate that the average area of the large pores is reduced from 703 μm^2 in Mix C0 to 44 μm^2 in Mix C30. Their average dimension is also decreased by 2.18–2.69 times after replacing 30% of and by DES. Different from Mix C0, some pores in Mix C30 were filled with fine aggregates. This results in higher bulk density, lower water absorption and better mechanical strengths of OPCCB with DES as discussed in the previous sections [55]. For the AASCB, fewer micro-pores are observed via comparing Mix C0 with Mix A0, which can be ascribed to the better packing condition of Mix A0 resulting from GGBS particles acting as micro-fillers [51]. This is also beneficial to enhancing the physical and mechanical properties of concrete blocks. Nonetheless, there are many micro-cracks existing in Mix A0 due to the shrinkage of alkali-activated materials, whilst they can hardly be observed in Mix A20. It can be deduced that the optimised packing status by incorporating DES possibly contributes to the prevention of micro cracks [56]. This eventually improves the physical and mechanical performances of AASCB containing DES. It can be inferred from Fig. 9(d) that AASCB with 20% DES shows the fewest micro cracks and pores, which can be recognised as the optimal mix formula for manufacturing concrete blocks.

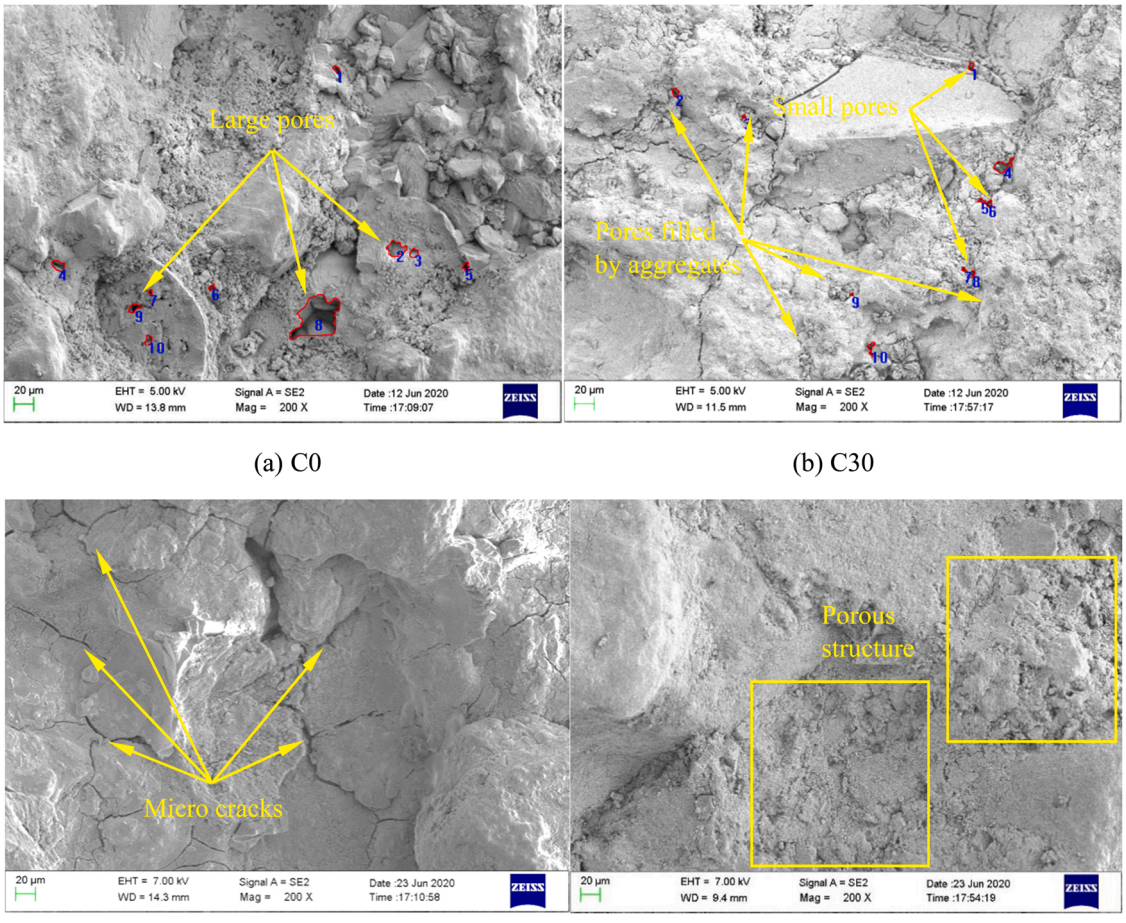

Fig. 11. SEM images of OPCCB and AASSB.

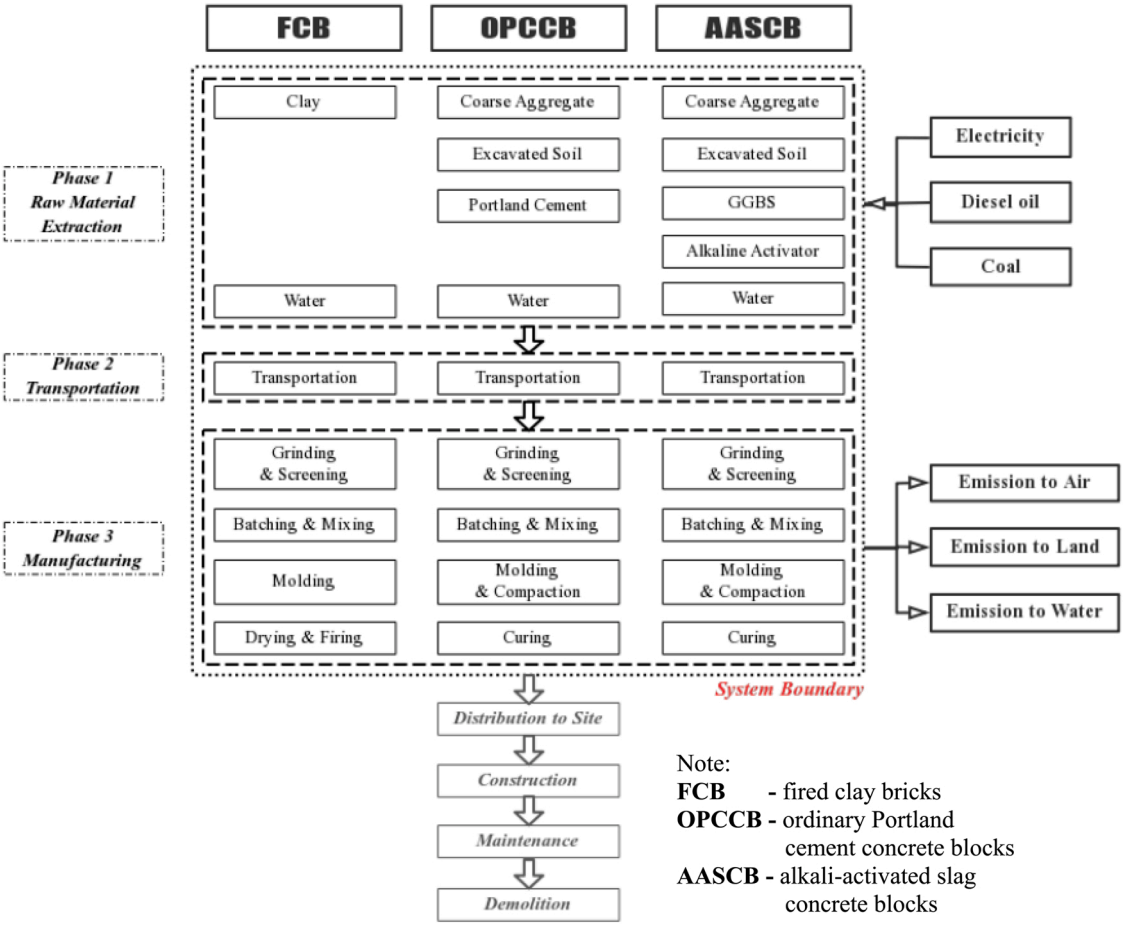

Fig. 12. Life cycle assessment of blocks.

Table 3
Statistics of pore sizes in mixes C0 and C30.

No.	C0			C30		
	Area (μm^2)	Length (μm)	Width (μm)	Area (μm^2)	Length (μm)	Width (μm)
1	143	17.01	9.79	35	7.85	5.03
2	743	38.16	30.06	49	9.04	7.39
3	229	17.48	16.65	15	4.51	3.99
4	374	29.20	18.64	164	23.51	12.92
5	138	15.54	12.75	27	8.46	4.52
6	114	13.65	11.03	39	8.48	6.42
7	70	12.35	7.80	19	6.69	3.25
8	4766	114.18	78.31	24	7.50	4.21
9	255	26.35	15.45	9	3.68	2.46
10	202	19.13	12.33	54	14.54	7.50
Ave.	703	30.30	21.28	44	9.53	5.77

4. Life cycle assessment (LCA)

4.1. System boundary and functional unit

Prior to data collection, a system boundary was established to demarcate the entire life cycle. Normally, a cradle-to-grave life cycle of blocks consists of seven phases as shown in Fig. 12, including acquisition of crude materials, transportation to factories, manufacture of products, distribution to construction sites, construction, maintenance, and terminus of its service life. However, the phases after product manufacturing were barely considered in LCA as the energy consumed and the carbon emitted can be presumed equivalent.

Hence, this study is aimed at the first three phases of concrete blocks (i.e. from cradle to gate). The energy consumption (EC) and global warming potential (GWP) of concrete blocks were quantified and analysed. To make the LCA results comparable among the three types of concrete blocks, 1 m^3 was selected as the functional unit, based on which all the numerical analyses would be conducted. Furthermore, it was assumed that the functional unit was completely separated from the others, suggesting that there was no mortar or paste existing between the adjacent blocks. The study refers to the direct energy of the raw materials and those consumed in the processes from extraction to manufacture. The indirect energy associated with the infrastructures was not considered.

4.2. Data sources

4.2.1. Raw materials

Energy is required for raw material exploitation. Fire clay bricks (FCB) was composed of 90% naturally quarried clay together with 10% water by mass [57]. Venta et al. [3] pointed out that extracting a ton of clay consumes 1.14 L diesel. Assuming the energy density of diesel is 35.8 MJ/L [2], the EC for clay acquisition can be calculated as 0.041 MJ/kg. The EC of water is assumed to be 0.001 MJ/kg [2]. For OPCCB and AASCB, the fine and coarse aggregates were natural river sand and crushed gravels. The exploitation of sand and crushed gravels demands 0.23 MJ/kg and 0.35 MJ/kg embodied energy, respectively [58]. The energy consumed for extracting DES was considered to be 0 MJ/L, as it should have been disposed at landfills. Utilizing it as a construction material can avoid landfilling with machinery, which can save energy required for disposal. This beneficial effect can be counted to be 0.014 MJ/kg according to the study of Xiao et al. [59]. For the binder in OPCCB, the EC of cement was taken as 4.8 MJ/kg, which is averaged from the recommended values in the two existing studies [60,61]. For AASCB, GGBS, as a residue of pig iron smelting, consumes 1.59 MJ/kg energy due to the post-treatment before its usage [62,63]. Based on the previous data [62,64], the energy expended for producing sodium hydroxide and sodium silicate were taken as 6.51 MJ/kg and 8.39 MJ/kg, respectively. It is worth noting that GWP values were calculated through multiplying the EC values in Table 3 with the carbon emission coefficients of different fuel categories listed in standard CECS 374:2014 [42]. Different from the other raw materials, cement manufacture generally causes prodigious carbon emissions, so its GWP was separately considered to be 1.07 kg CO_2-eq/kg based on the previous studies [60,61].

4.2.2. Transportation

Shipping materials by a Class 7 dump truck would consume 52 L diesel per 1000 t-km [65]. The freight distance for all the raw materials and DES disposal was assumed to be 50 km for a one–way conveyance. Moreover, its EC value was calculated to be 0.092 MJ/kg for one way transportation in light of the energy intensity of diesel [2]. As reusing DES is able to save energy, the energy saved in transportation was considered as 0.092 MJ/kg.

4.2.3. Manufacture

In the manufacturing process of FCB, EC of preparatory work and block moulding was assumed to be 1.93 MJ/kg [3], while that of drying and firing processes was 2.835 MJ/kg [2]. The EC value of the drying and firing processes was found to be consistent with that suggested by Athena™ [3]. Both OPCCB and AASCB were produced in similar technical procedure [66]. This process consisting of grinding, screening, batching, mixing, moulding would consume the embodied energy of 0.7 MJ/kg [2]. In this study, the equipment for block manufacturing was powered by a hydraulic motor with a rated capacity factor of 22.4 kW [61], leading to the EC value of 0.013 MJ/kg. There is no additional energy for curing as they were demoulded and cured at room temperature.

4.2.4. Life cycle inventory

The embodied energies of the first three phases in block production are summarised in Table 4. To obtain the integral energy

Table 4
Energy consumed from Phase I to Phase III.

Procedure	Unit	FCB	OPCCB	AASCB
Phase I: acquisition				
DES	MJ/kg	N/A	0	0
Clay	MJ/kg	0.041	N/A	N/A
Fine aggregate	MJ/kg	N/A	0.023	0.023
Coarse aggregate	MJ/kg	N/A	0.035	0.035
Water	MJ/kg	0.001	0.001	0.001
OPC	MJ/kg	N/A	4.8	N/A
Slag	MJ/kg	N/A	N/A	1.589
Sodium hydroxide	MJ/kg	N/A	N/A	6.508
Sodium silicate	MJ/kg	N/A	N/A	8.390
Landfill avoidance	MJ/kg	N/A	-0.014	-0.014
Phase II: transportation				
Material conveyance	MJ/kg	0.092	0.092	0.092
Avoidance of landfilling	MJ/kg	N/A	-0.092	-0.092
Phase III: manufacture				
Processing	MJ/kg	1.930	0.7	0.7
Drying & firing	MJ/kg	2.835	N/A	N/A
Compaction	MJ/kg	N/A	0.013	0.013

consumption, the values below were multiplied by the material proportion prescribed in Table 2.

4.3. Energy consumption (EC)

Fig. 13 demonstrates the embodied energy within the LCA boundaries of FCB, OPCCB and AASCB. It is readily seen that the overall EC values of the OPCCB and AASCB are 72.1% and 72.8% lower than that of FCB, respectively. This is mainly caused by the high energy consumption in manufacturing process for FCB. As seen in Fig. 11, the manufacturing process dominantly takes up 97% of the entire life-cycle energy for FCB. This ratio is reduced to 59.0% and 64.9% for OPCCB and AASCB, respectively. This transformation of the fabrication method from firing to compaction enables enormous energy saving [67]. Moreover, the manufacturing manner of OPCCB and AASCB is free of initial curing, which has been proven to benefit the environment [61]. However, the processing takes up over 50% of total energy consumption for both OPCCB and AASCB, suggesting its potential of further optimisation in the future. The EC of AASCB is slightly lower than that of OPCCB, which is mainly attributed to the higher extraction EC of OPCCB (i.e., 908.69 MJ) due to the use of cement. In contrast, the EC resulting from the AAS binder accounts for 668.76 MJ. It can be found that the unit EC of AAS (2.757 MJ/kg) is reduced by 42.56% as compared to OPC (4.800 MJ/kg). As reported in [61], Na_2SiO_3 in form of spray powder would consume more energy than that in form of hydrothermal liquor. Similarly, producing NaOH via the diaphragm cell method would consume more energy than the membrane cell method. Therefore, the energy consumption of AASCB can be further reduced through the optimisation of alkali activators. Moreover, the use of industrial by-products from muriatic acid manufacturing, sulphuric acid neutralisation [68] and desalination [69] as the alkali activators can also provide a novel way for energy conservation of AAS.

4.4. Global warming potential (GWP)

GWP is a climate-change-related indicator depicting the capacity of a product or procedure in warming up the earth atmosphere. Herein, the CO_2 equivalent (abbreviated as CO_2-eq) was utilised as a benchmark to evaluate the overall warming efficacy of the three types of blocks [70]. Fig. 14 presents the CO_2 equivalents of FCB, OPCCB (C30) and AASCB (AA20). In general, the CO_2 equivalents of OPCCB and AASCB are much lower than that of FCB. For instance, the CO_2 equivalent of concrete blocks is around one third of that of FCB. This is mainly attributed to the high carbon emission in the sintering process for FCB manufacturing. This is consistent with the findings reported by Habert et al. [71]. Moreover, CO_2 equivalent of AASCB is 13.7% lower than that of OPCCB due to the adoption of different binders. For OPCCB, the use of OPC raises CO_2 equivalent to 201.62 kg, which accounts for 97.3% of the total GWP of its Phase I. This is mainly caused by the fuel combustion and pyrolysis of the raw materials, which is estimated to be 0.52 kg CO_2-eq for 1 kg of cement production [72]. Besides, the released sulphur dioxide (SO_2) and nitrogen oxides (NO_x) further increase the carbon equivalent [73]. The AAS binder in AASCB contributes 89.92 kg CO_2-eq, accounting for 91.1% of the whole GWP in Phase I. The unit GWP of AAS equals to 0.37 kg CO_2-eq/kg, which is 65.4% lower than that of OPC (i.e., 1.07 kg CO_2-eq/kg). In AASCB, sodium silicate (Na_2SiO_3) accounts for 57.0% of the total emission of this phase, which is higher than the sodium hydroxide (24.11%) due to the higher unit carbon emission of sodium silicate. Overall, AAS could be considered as a cleaner binder in block industry in contrast with OPC. Furthermore, the manufacturing procedure leads to most of the CO_2 emissions in the entire life cycle for both OPCCB (59.39%) and AASCB (75.30%), which means more efforts can be made on optimising the manufacture technique to reduce the GWP.

Carbon intensity index (CII) and binder intensity index (BII) are calculated based on the mechanical and environmental performances of blocks as shown in Table 5. The CII, defined as the carbon equivalent generated per unit of compressive strength, denotes the environmental friendliness of the product [74]. The BII, expressed as a mass ratio of the binder to the compressive strength, intends to characterise the efficiency of the binders. AASCB exhibits the lowest CII, which is 86.2% and 62.2% lower than FCB and OPCCB, respectively. Consequently, it can be readily deduced that AASCB has the lowest carbon emission retrenchment at a given mechanical

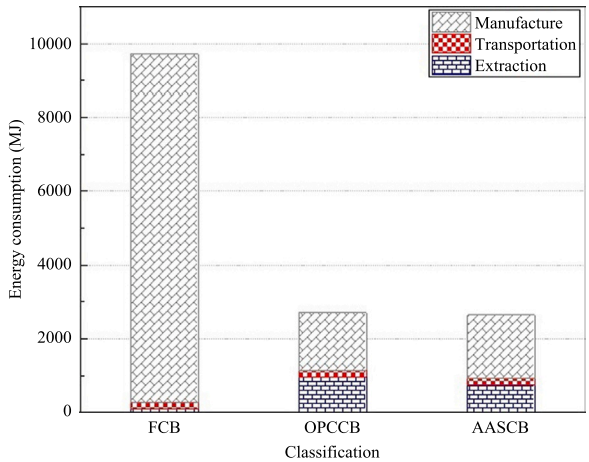

Fig. 13. Energy consumption.

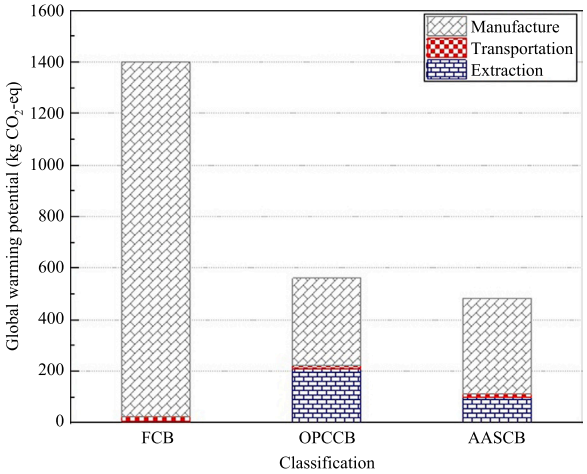

Fig. 14. Global warming potentials.

Table 5
Intensity indices.

Category	Unit	FCB	OPCCB (C30)	AASCB (A20)
CII	kg CO_2-eq m^{-3} MPa^{-1}	70.06	25.51	9.64
BII	kg binder m^{-3} MPa^{-1}	–	8.63	4.84

strength. The comparison of BII values demonstrates that AASCB requires less binder than OPCCB to achieve the same compressive strength. Hence, AAS could be recommended as a promising green cementitious material in manufacturing concrete blocks.

5. Conclusions

This paper studied the engineering properties and sustainability of OPC and AAS concrete blocks containing dewatered extracted soil (DES) as fine aggregate. The physical and mechanical properties of concrete blocks with different amounts of soil were measured and compared. The life cycle assessment was also performed to estimate the energy consumption and carbon emission of the blocks. The following conclusions can be drawn based on the test results and analysis.

(1) Increasing the DES content first increase the bulk density and decrease the water absorption of concrete blocks produced with AAS or OPC, which is mainly attributed to the densification of structure by the fine soil particles. However, excessive soil decreases the bulk density and increases the water absorption of concrete blocks due to the voids created by the agglomerated soils.
(2) The use of DES can improve the packing status of aggregates and subsequently enhances the compressive strength and flexural strength of concrete blocks produced with OPC or AAS. However, the addition of excessive soils decreases the strength of concrete blocks as more OPC or AAS are required to bind and coat the aggregates.
(3) Life cycle assessment indicates that OPCCB and AASCB exhibit 72% and 60% lower energy consumption and carbon emission as compared to fired clay bricks, respectively. Moreover, AASCB shows lower carbon intensity index and binder intensity index as compared to OPCCB, indicating that AASCB is a promising alternative block considering both the environmental benefits and mechanical performances.

Declaration of Competing Interest

The authors declare that they have no known competing financial interests or personal relationships that could have appeared to influence the work reported in this paper.

Acknowledgements

The authors wish to acknowledge the financial support from the Ningbo Municipal Bureau of Science and Technology under Commonweal Programme (No.: 2021S097) and CM2025 programme (No.: 2019B10048), and Zhejiang Key R&D Project (No.: 2021C03162). The Zhejiang Provincial Department of Science and Technology is acknowledged for this research under its Provincial Key Laboratory Programme (No.: 2020E10018).

References

[1] L. Zhang, Production of bricks from waste materials – a review, Constr. Build. Mater. 47 (2013) 643–655.
[2] S. Bhairappanavar, R. Liu, A. Shakoor, Eco-friendly dredged material-cement bricks, Constr. Build. Mater. 271 (2021), 121524, https://doi.org/10.1016/j.conbuildmat.2020.121524.
[3] G.J. Venta, P. Eng, Life cycle analysis of brick and mortar products, Athena [TM] Sustainable Materials Institute, Ottawa, Canada, 1998.
[4] A. Arulrajah, M.M. Disfani, S. Horpibulsuk, C. Suksiripattanapong, N. Prongmanee, Physical properties and shear strength responses of recycled construction and demolition materials in unbound pavement base/subbase applications, Constr. Build. Mater. 58 (2014) 245–257, https://doi.org/10.1016/j.conbuildmat.2014.02.025.
[5] A. Kumar Suluguru, M. Jayatheja, A. Kar, A. GuhaRay, S.R. Surana, N. James, Experimental studies on the microstructural, physical and chemical characteristics of building derived materials to assess their suitability in ground improvement, Constr. Build. Mater. 156 (2017) 921–932, https://doi.org/10.1016/j.conbuildmat.2017.09.058.
[6] A.K. Suluguru, S.R. Surana, A. GuhaRay, A. Kar, J. Muktinutalapati, Experimental investigations on building derived materials in chemically aggressive environment as a partial replacement of soil in geotechnical applications, Geotech. Geol. Eng. 37 (2019) 947–963, https://doi.org/10.1007/s10706-018-0662-0.
[7] J. Chen, M. Sanger, R. Ritchey, T.B. Edil, M. Ginder-Vogel, Neutralization of high pH and alkalinity effluent from recycled concrete aggregate by common subgrade soil, J. Environ. Qual. 49 (2020) 172–183, https://doi.org/10.1002/jeq2.20008.
[8] C.S. Poon, S.C. Kou, L. Lam, Use of recycled aggregates in molded concrete bricks and blocks, Constr. Build. Mater. 16 (2002) 281–289.
[9] Z. Zhao, L. Courard, S. Groslambert, T. Jehin, A. Léonard, J. Xiao, Use of recycled concrete aggregates from precast block for the production of new building blocks: an industrial scale study, Resour. Conserv. Recycl. 157 (2020), 104786.
[10] A. Karimipour, M. Edalati, Influence of untreated coal and recycled aggregates on the mechanical properties of green concrete, J. Clean. Prod. 276 (2020), 124291.
[11] B.M.V. Kumar, H. Ananthan, K.V.A. Balaji, Experimental studies on cement stabilized masonry blocks prepared from brick powder, fine recycled concrete aggregate and pozzolanic materials, J. Build. Eng. 10 (2017) 80–88, https://doi.org/10.1016/j.jobe.2017.02.007.
[12] M. Haas, R. Galler, L. Scibile, M. Benedikt, Waste or valuable resource – a critical European review on re-using and managing tunnel excavation material, Resour. Conserv. Recycl. 162 (2020), 105048, https://doi.org/10.1016/j.resconrec.2020.105048.
[13] J. Meegoda, A.S. Ezeldin, D.A. Vaccari, R.T. Mueller, Petroleum contaminated soils in highway construction, in: Infrastructute: New Materials and Methods of Repair, ASCE, 1994, pp. 904–911.
[14] A.W. Hago, H.F. Hassan, A. Al Rawas, R. Taha, S. Al-Hadidi, Characterization of concrete blocks containing petroleum-contaminated soils, Constr. Build. Mater. 21 (2007) 952–957, https://doi.org/10.1016/j.conbuildmat.2006.04.006.
[15] V. Lesovik, A. Volodchenko, R. Fediuk, Y.H. Mugahed Amran, R. Timokhin, Enhancing performances of clay masonry materials based on nanosize mine waste, Constr. Build. Mater. 269 (2021), 121333, https://doi.org/10.1016/j.conbuildmat.2020.121333.
[16] A.C.J. de Korte, H.J.H. Brouwers, Production of non-constructive concrete blocks using contaminated soil, Constr. Build. Mater. 23 (2009) 3564–3578.
[17] B.V. Venkatarama Reddy, A. Gupta, Influence of sand grading on the characteristics of mortars and soil–cement block masonry, Constr. Build. Mater. 22 (2008) 1614–1623.
[18] V. Sousa, J.A. Bogas, Comparison of energy consumption and carbon emissions from clinker and recycled cement production, J. Clean. Prod. 306 (2021), 127277.
[19] Y. Gu, H. Cao, W. Liu, X. Lin, T. Zheng, W. Cheng, J. Huang, J. Xu, Impact of co-processing sewage sludge on cement kiln NOx emissions reduction, J. Environ. Chem. Eng. 9 (2021), 105511.
[20] J. Davidovits, Geopolymers: ceramic-like inorganic polymers, J. Ceram. Sci. Technol. 80 (2017) 335–350, https://doi.org/10.4416/JCST2017-00038.
[21] D. Hardjito, S.E. Wallah, D.M. Sumajouw, B.V. Rangan, Fly ash-based geopolymer concrete, Aust. J. Struct. Eng. 6 (2005) 1–19.
[22] B.V. Rangan, Geopolymer concrete for environmental protection, Indian Concr. J. 88 (2014) 41–59.
[23] D. Hardjito, S.E. Wallah, D.M.J. Sumajouw, B.V. Rangan, On the development of fly ash-based geopolymer concrete, ACI Mater. J. 101 (2004) 467–472.
[24] Z. Li, T. Lu, X. Liang, H. Dong, G. Ye, Mechanisms of autogenous shrinkage of alkali-activated slag and fly ash pastes, Cem. Concr. Res. 135 (2020), 106107, https://doi.org/10.1016/j.cemconres.2020.106107.
[25] K.K. Ramagiri, A. Kar, Effect of high-temperature on the microstructure of alkali-activated binder, Mater. Today Proc. 28 (2020) 1123–1129, https://doi.org/10.1016/j.matpr.2020.01.093.
[26] K.K. Ramagiri, D.R. Chauhan, S. Gupta, A. Kar, D. Adak, A. Mukherjee, High-temperature performance of ambient-cured alkali-activated binder concrete, Innov. Infrastruct. Solut. 6 (2021) 1–11, https://doi.org/10.1007/s41062-020-00448-y.
[27] K.K. Ramagiri, D. Chauhan, S. Gupta, A. Kar, D. Adak, Evaluation of structural performance of concrete with ambient-cured alkali-activated binders, in: K. Dasgupta, A.S. Sajith, G. Unni Kartha, A. Joseph, P.E. Kavitha, K.I. Praseeda (Eds.), Proceedings of SECON'19, Springer International Publishing, Cham, 2020, pp. 1–10, https://doi.org/10.1007/978-3-030-26365-2_1.
[28] Z. Li, M. Nedeljković, B. Chen, G. Ye, Mitigating the autogenous shrinkage of alkali-activated slag by metakaolin, Cem. Concr. Res. 122 (2019) 30–41, https://doi.org/10.1016/j.cemconres.2019.04.016.
[29] K.K. Ramagiri, S.Y. Kudumala, R. Chintha, A. Kar, Drying shrinkage of alkali-activated paste, mortar and concrete—a comparison study for varying activator modulus, in: SECON 2021, Lecture Notes in Civil Engineering, Springer, Cham, 2021, pp. 551–557.
[30] R.K. Preethi, B.V. Venkatarama Reddy, Experimental investigations on geopolymer stabilised compressed earth products, Constr. Build. Mater. 257 (2020), 119563.
[31] K.K. Ramagiri, R. Chintha, R.K. Bandlamudi, P. Kara De Maeijer, A. Kar, Cradle-to-gate life cycle and economic assessment of sustainable concrete mixes—alkali-activated concrete (AAC) and bacterial concrete (BC), Infrastructures 6 (2021) 104, https://doi.org/10.3390/infrastructures6070104.
[32] H.R. Gavali, A. Bras, P. Faria, R.V. Ralegaonkar, Development of sustainable alkali-activated bricks using industrial wastes, Constr. Build. Mater. 215 (2019) 180–191.
[33] M.M.A. Abdullah, W.M.W. Ibrahim, M.F.M. Tahir, The properties and durability of fly ash-based geopolymeric masonry bricks, in: F. Pacheco-Torgal, P.B. Lourenço, J.A. Labrincha, S. Kumar, P. Chindaprasirt (Eds.), Eco-Efficient Masonry Bricks and Blocks, Woodhead Publishing, Oxford, 2015: pp. 273–287.
[34] P. Ren, B. Li, J.-G. Yu, T.-C. Ling, Utilization of recycled concrete fines and powders to produce alkali-activated slag concrete blocks, J. Clean. Prod. 267 (2020), 122115.
[35] GB/T 175: Ordinary Portland Cement, Chinese Standards Association, 2007.
[36] GB/T 18046: Ground granulated blast furnace slag used for cement, mortar and concrete, Chinese Standards Association, 2017.
[37] BS EN ISO 14688-2:2004 Geotechnical investigation and testing - Identification and classification of soil - Part 2: Principles for a classification, British Standards Institution, London, England, 2004.
[38] JTG 3430-2020 Test Methods of Soils for Highway Engineering, Ministry of Transport of China, China, 2020.
[39] GB/T 14684:2011 Sand for construction, Chinese Standards Association, China, 2011.
[40] M. Kawamura, Y. Kasai, Determination of saturated surface-dry condition of clay–sand mixed soils for soil–cement concrete construction, Mater. Struct. 43 (2010) 571–582.
[41] ASTM C642-2013: Standard test method for density, absorption, and voids in hardened concrete, ASTM International, 2013.
[42] ISO 14040: 2006 Environmental Management - Life Cycle Assessment - Principles and Framework, International Organisation for Standardisation, 2006.
[43] ISO 14044: 2006 Environmental Management - Life Cycle Assessment - Requirements and Guidelines, International Organisation for Standardisation, 2006.
[44] A.P. Vilela, T.M.C. Eugênio, F.F. de Oliveira, J.F. Mendes, A.G.C. Ribeiro, L.E.V. de, S. Brandão Vaz, R.F. Mendes, Technological properties of soil-cement bricks produced with iron ore mining waste, Constr. Build. Mater. 262 (2020), 120883.

[45] S.H. Chu, C.S. Poon, C.S. Lam, L. Li, Effect of natural and recycled aggregate packing on properties of concrete blocks, Constr. Build. Mater. 278 (2021), 122247, https://doi.org/10.1016/j.conbuildmat.2021.122247.
[46] F.B. Siqueira, J.N.F. Holanda, Reuse of grits waste for the production of soil–cement bricks, J. Environ. Manag. 131 (2013) 1–6.
[47] H.-M. Kwon, A.T. Le, N.T. Nguyen, Influence of soil grading on properties of compressed cement-soil, KSCE J. Civ. Eng. 14 (2010) 845–853.
[48] P.J. Walker, Strength, durability and shrinkage characteristics of cement stabilised soil blocks, Cem. Concr. Compos. 17 (1995) 301–310, https://doi.org/10.1016/0958-9465(95)00019-9.
[49] D.D. Tripura, K.D. Singh, Characteristic properties of cement-stabilized rammed earth blocks, J. Mater. Civ. Eng. 27 (2015), 04014214.
[50] R. Bahar, M. Benazzoug, S. Kenai, Performance of compacted cement-stabilised soil, Cem. Concr. Compos. 26 (2004) 811–820.
[51] T.E. Elahi, A.R. Shahriar, M.S. Islam, Engineering characteristics of compressed earth blocks stabilized with cement and fly ash, Constr. Build. Mater. 277 (2021), 122367, https://doi.org/10.1016/j.conbuildmat.2021.122367.
[52] P. Shoaei, F. Ameri, H. Reza Musaeei, T. Ghasemi, C.B. Cheah, Glass powder as a partial precursor in Portland cement and alkali-activated slag mortar: a comprehensive comparative study, Constr. Build. Mater. 251 (2020), 118991.
[53] E. Hany, N. Fouad, M. Abdel-Wahab, E. Sadek, Compressive strength of mortars incorporating alkali-activated materials as partial or full replacement of cement, Constr. Build. Mater. 261 (2020), 120518.
[54] M.S. Islam, T.E. Elahi, A.R. Shahriar, N. Mumtaz, Effectiveness of fly ash and cement for compressed stabilized earth block construction, Constr. Build. Mater. 255 (2020), 119392.
[55] T.E. Elahi, A.R. Shahriar, M.S. Islam, F. Mehzabin, N. Mumtaz, Suitability of fly ash and cement for fabrication of compressed stabilized earth blocks, Constr. Build. Mater. 263 (2020), 120935, https://doi.org/10.1016/j.conbuildmat.2020.120935.
[56] P. Perumal, H. Sreenivasan, T. Luukkonen, A.M. Kantola, V.-V. Telkki, P. Kinnunen, M. Illikainen, High strength one-part alkali-activated slag blends designed by particle packing optimization, Constr. Build. Mater. 299 (2021), 124004.
[57] O. Gencel, E. Erdugmus, M. Sutcu, O.H. Oren, Effects of concrete waste on characteristics of structural fired clay bricks, Constr. Build. Mater. 255 (2020), 119362.
[58] M.A. Nisbet, M.G. VanGeem, J. Gajda, M. Marceau, Environmental life cycle inventory of portland cement concrete, Portland Cement Association, Skokie, Illinois, 2000.
[59] J. Xiao, Y. Xiao, Y. Liu, T. Ding, Carbon emission analyses of concretes made with recycled materials considering CO_2 uptake through carbonation absorption, Struct. Concr. 22 (2021) 58–73, https://doi:10.1002/suco.201900577.
[60] NREL: U.S. Life Cycle Inventory Database, National Renewable Energy Laboratory, 2012.
[61] J. Dahmen, J. Kim, C.M. Ouellet-Plamondon, Life cycle assessment of emergent masonry blocks, J. Clean. Prod. 171 (2018) 1622–1637, https://doi.org/10.1016/j.jclepro.2017.10.044.
[62] J.F. Rivera, R. Mejía de Gutiérrez, S. Ramirez-Benavides, A. Orobio, Compressed and stabilized soil blocks with fly ash-based alkali-activated cements, Constr. Build. Mater. 264 (2020), 120285, https://doi.org/10.1016/j.conbuildmat.2020.120285.
[63] A. Seco, J. Omer, S. Marcelino, S. Espuelas, E. Prieto, Sustainable unfired bricks manufacturing from construction and demolition wastes, Constr. Build. Mater. 167 (2018) 154–165.
[64] R. Robayo-Salazar, J. Mejía-Arcila, R. Mejía de Gutiérrez, E. Martínez, Life cycle assessment (LCA) of an alkali-activated binary concrete based on natural volcanic pozzolan: a comparative analysis to OPC concrete, Constr. Build. Mater. 176 (2018) 103–111.
[65] W. Harrington, Fuel Consumption Standards for Heavy Duty Vehicles, Resources, 2012.
[66] E.A. Adam, A.R.A. Agib, Compressed stabilised earth block manufacture in Sudan, United Nations Educational, Scientific and Cultural Organisation, Paris, France, 2001.
[67] B.V. Reddy, K. Jagadish, Embodied energy of common and alternative building materials and technologies, Energy Build. 352 (2003) 129–137.
[68] S.A. Bernal, Advances in near-neutral salts activation of blast furnace slags, RILEM Tech. Lett. 1 (2016) 39–44.
[69] V. Shkolnikov, S.S. Bahga, J.G. Santiago, Desalination and hydrogen, chlorine, and sodium hydroxide production via electrophoretic ion exchange and precipitation, Phys. Chem. Chem. Phys. 14 (2012) 11534–11545.
[70] D.-A. Chisalita, L. Petrescu, P. Cobden, H.A.J. (Eric) van Dijk, A.-M. Cormos, C.-C. Cormos, Assessing the environmental impact of an integrated steel mill with post-combustion CO_2 capture and storage using the LCA methodology, J. Clean. Prod. 211 (2019) 1015–1025.
[71] G. Habert, J.B. d'Espinose de Lacaillerie, N. Roussel, An environmental evaluation of geopolymer based concrete production: reviewing current research trends, J. Clean. Prod. 19 (2011) 1229–1238, https://doi.org/10.1016/j.jclepro.2011.03.012.
[72] M. Georgiopoulou, G. Lyberatos, Life cycle assessment of the use of alternative fuels in cement kilns: a case study, J. Environ. Manag. 216 (2018) 224–234.
[73] M. Schneider, M. Romer, M. Tschudin, H. Bolio, Sustainable cement production-present and future, Cem. Concr. Res. 41 (2011) 642–650.
[74] H. Van Damme, H. Houben, Earth concrete. Stabilization revisited, Cem. Concr. Res. 114 (2018) 90–102.